Available online at www.sciencedirect.com

ScienceDirect

*Mendeleev Commun.*, 2023, **33**, 817–820

Mendeleev Communications

# Adsorption of methane and ethane on HKUST-1 metal–organic framework and mesoporous silica composites

**Gregory S. Deyko,*[a] Lev M. Glukhov,[a] Vera I. Isaeva,[a] Vadim V. Vergun,[a] Vladimir V. Chernyshev,[b,c] Gennady I. Kapustin[a] and Leonid M. Kustov[a,b,d]**

[a] *N. D. Zelinsky Institute of Organic Chemistry, Russian Academy of Sciences, 119991 Moscow, Russian Federation. Fax: +7 916 161 3149; e-mail: gdeyko@gmail.com*
[b] *Department of Chemistry, M. V. Lomonosov Moscow State University, 119991 Moscow, Russian Federation*
[c] *A. N. Frumkin Institute of Physical Chemistry and Electrochemistry, Russian Academy of Sciences, 119071 Moscow, Russian Federation*
[d] *National University of Science and Technology 'MISIS', 119049 Moscow, Russian Federation*

DOI: 10.1016/j.mencom.2023.10.026

**Composite materials HKUST-1@MCM-41 and HKUST-1@BPS based on metal–organic framework HKUST-1 [$Cu_3(btc)_2$, btc = benzene-1,3,5-tricarboxylate] and silicas, *i.e.*, mesoporous MCM-41 and biporous BPS with a bimodal mesopore size distribution, were prepared by one-step direct growth technique. Methane and ethane adsorption isotherms were measured for the HKUST-1@MCM-41 and HKUST-1@BPS composites in a wide pressure range for the first time. The silica porous structure significantly affects the content and location of HKUST-1 crystallites in these host matrices, and thereby the adsorption selectivities of the composites.**

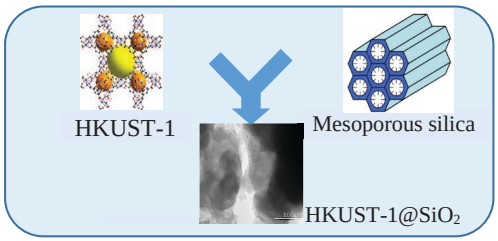


*Keywords*: hybrid materials, metal–organic frameworks, mesoporous silica, adsorption, methane, ethane.

*Dedicated to M. Egorov who merged physical chemistry and organic chemistry into a hybrid monolyth (something like MOF) and paved the way for the future of Institute of Organic Chemistry.*

Natural gas is a mixture of gases, mainly methane (50–90%) and other lower alkanes, *e.g.*, ethane (3–20%), which is a valuable industrial feedstock. Therefore, the development of energy-efficient methods for ethane separation from natural gas are highly demanded. One of the most promising strategies for this purpose is adsorption on nanoporous solids, *e.g.*, zeolites, silicas and carbon-based materials.[1,2] Nevertheless, despite the achievements in tuning their separation performance,[3] increasing the selectivity and capacity of modern adsorbents remains a challenge.

In this context, a novel class of hybrid crystalline coordination polymers, metal–organic frameworks (MOFs) composed of metal cations and polyfunctional organic molecules (linkers), has a significant potential for adsorption of natural gas components, including methane and ethane,[4] *e.g.*, HKUST-1 [$Cu_3(btc)_2$],[5,6] SBMOF-1 [Ca(SDB), SDB = 4,4′-sulfonyldibenzoate],[7] DUT-8 [$M(2,6\text{-NDCA})(TED)_{0.5}$, 2,6-NDCA = 2,6-natphthalene-dicarboxylate, TED = 1,4-diazabicyclo[2.2.2]octane],[8] DUT-75 [$Cu_3(CPCDC)_2(H_2O)_x(DMF)_y(EtOH)_z$, CPCDC = 9-(4-carboxylatophenyl)-9*H*-carbazole-3,6-dicarboxylate][9] and DUT-49 [$Cu_2$(BBCDC), BBCDC = 9,9′-([1,1′-biphenyl]-4,4′-diyl)bis(9*H*-carbazole-3,6-dicarboxylate)].[10] In particular, it was found in a series of DUT-8 (M = Co, Ni, Cu, and Zn) materials that the rigid frameworks DUT-8 (Cu, Ni) exhibit an outstanding $C_2H_6$ uptake (up to 11.2 mmol $g^{-1}$, 283–303 K, 10 bar), due to the C–H···π interaction close to the metal node (as an adsorption site).[8]

However, only methane adsorption data have been published for the most of reported MOF matrices. So, the DUT-75 matrix shows the methane capacity of ~ 240 mg $g^{-1}$ (298 K, 90 atm), while, the record-breaking value of 308 mg $g^{-1}$ under the same conditions is achieved for the DUT-76 adsorbent.[9] Zn(SDB) (an isostructural analog of SBMOF-1) shows methane and ethane adsorption capacities of 4.9 mg $g^{-1}$ and 20 mg $g^{-1}$ (298 K, 1 atm), respectively.[11] The ideal selectivity for this adsorbent calculated by the ideal adsorbed solution theory (IAST) method is 23.2 : 1 (298 K, 1 atm) in separation of the equimolar $C_2H_6/CH_4$ mixture. The HKUST-1 material prepared by the solvothermal method demonstrates the methane adsorption capacity of ~ 4.5 mmol $g^{-1}$ (303 K, 10 bar)[5] and the ethane adsorption capacity of ~ 3.5 mmol $g^{-1}$ (313 K, 1 bar).[12] This matrix is a promising adsorbent for the separation of the natural gas components due to its high methane and ethane adsorption capacities. Moreover, it can be synthesized by different methods[13] and with a relatively low production expenses as compared to other MOF-based adsorbents, *e.g.*, DUT-8 and DUT-75.

Mesoporous silicas, *e.g.*, MCM-41, SBA-15, KIT-5, and COK-12, represent another type of highly ordered adsorbents. Like MOF materials, these inorganic supports have a three-dimensional framework with a high specific surface area (400–1500 $m^2$ $g^{-1}$). Currently, mesoporous silicas are used as components for heterogeneous catalysts,[14] in drug delivery systems,[15] as well as adsorbents for natural gas treatment[16] and volatile organic compounds capturing.[17] However, methane and ethane adsorption data are known only for MCM and SBA matrices. In particular, the adsorption of methane and ethane on MCM-41 was explored in wide pressure and temperature ranges.[18] The methane and ethane adsorption capacities of this

material are 2 mmol $g^{-1}$ and 6 mmol $g^{-1}$ (30 °C, 25 atm), respectively. For SBA-15, the adsorption values are 0.1 mmol $g^{-1}$ for methane, and 0.6 mmol $g^{-1}$ for ethane under the same conditions (30 °C, 1.3 atm).[19]

The preparation of composites based on MOF crystals and mesoporous silicas is a promising strategy in the development of different adsorbents.[20] MOF@silica composites have been examined in gas adsorption (mainly for $CO_2$ sequestration).[21] However, there are no data on their use in the separation of methane from ethane.

Recently, an impact of the synthesis procedure on the textural properties and crystal size of the microporous HKUST-1 materials has been reported, which remarkably affects the adsorption capacities and ideal selectivity for the methane–ethane pair.[22] The aim of this work was to elucidate an effect of the hierarchical porous structure of the materials based on HKUST-1 on their performance in selective ethane/methane adsorption. To this end, the functional composites based on HKUST-1 nanocrystals and mesoporous silicas, *i.e.*, MCM-41 (a monomodal mesopore size distribution) and BPS (biporous silica with a bimodal mesopore size distribution), were synthesized. The ideal selectivities of the HKUST-1@MCM-41 and HKUST-1@BPS composites in the adsorption processes of methane and ethane were evaluated in a wide pressure range, which is important from the practical point of view.

The HKUST-1@MCM-41 and HKUST-1@BPS composites were prepared according to the one-step approach, which involved the formation of HKUST-1 crystallites in silica pores under solvothermal conditions. According to elemental analysis (see Online Supplementary Materials, Table S1), the HKUST-1 content is 18.8 wt% for the HKUST-1@MCM-41 material and 26.3 wt% for the HKUST-1@BPS sample. This difference could be explained by various pore dimensions in MCM-41 and BPS matrices. So, the BPS adsorbent with a fraction of large mesopores (Table S2) is capable to accommodate much more HKUST-1 crystallites as compared to its MCM-41 analog.

The presence of the HKUST-1 crystalline phase in the resulting composites was confirmed by the powder XRD data (Figure 1).

The PXRD data indicate that almost all the main reflections in the diffraction patterns of the composites have a reduced intensity compared to the reference HKUST-1 sample [Figure 1(*a*)]. It also can be seen that the HKUST-1 phase in the composites does not undergo any significant changes. Despite the redistribution of the intensities of the main diffraction peaks caused by small changes in porosity, the cubic cell parameter *a* does not change, corresponding to 26.371(2) Å in the reference HKUST-1 sample and 26.370(2) Å in the HKUST-1@BPS composite. Two strong Bragg peaks in the low-angle range of $2\theta$ = 3–5° in the diffraction pattern of the HKUST-1@MCM-41 sample [Figure 1(*b*)] are due to the mesoporous structure of the highly ordered matrix MCM-41. In the case of an X-ray amorphous BPS material, this low-angle range is covered by the intense small-angle scattering from the nanosized particles of the amorphous matrix [Figure 1(*c*)].

The $N_2$ adsorption isotherms obtained for the HKUST-1@MCM-41 and HKUST-1@BPS materials display the same shape as the corresponding silica matrices. The investigated materials demonstrate type IV adsorption isotherms typical for mesoporous matrices except the microporous HKUST-1 reference sample showing a type I isotherm. However, a decreased $N_2$ uptake observed for the composites as compared to pristine silicas, is due to the partial pore blocking of the inorganic hosts by HKUST-1 crystallites.

The differences in porous structures of the obtained materials are observed in the curves of the micropore (Figure S2) and

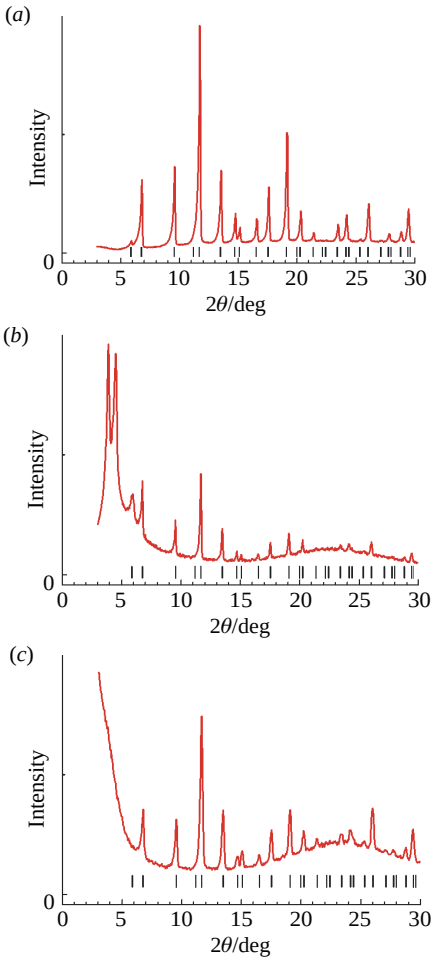


**Figure 1** Experimental diffraction patterns of (*a*) HKUST-1 material and composites (*b*) HKUST-1@MCM-41 and (*c*) HKUST-1@BPS.

mesopore (Figure S3) size distribution. The micropore size distribution for the HKUST-1 reference sample shows a main maximum at 0.6 nm. The curves of the mesopore size distributions have maxima almost at the same positions, *i.e.*, around 0.5 nm. At the same time their heights are significantly decreased as compared to those obtained for the pristine HKUST-1 material, and correlate with its content in the composites. The mesopore size distribution curves for the composite adsorbents are similar to those obtained for mesoporous silicas (Figure S3). A decrease in the mesopore diameter and volume is observed for both composites, which could be explained by the formation of HKUST-1 crystallites in pores of both MCM-41 and BPS matrices.

The MCM-41 matrix has a much higher specific surface area (BET), than its BPS counterpart. The differences in their pore structures are also observed (Table S2). The mesopore volume of the BPS material having a bimodal pore size distribution is almost twice as high than that obtained for the MCM-41 silica. The resulting composites have a lower specific surface area and total pore volume as compared to the HKUST-1 reference sample. The specific surface area and total pore volume of the HKUST-1@MCM-41 material are decreased compared with the parent MCM-41 matrix, while even a slight gain of the specific surface area is observed for the HKUST-1@BPS system. However, a total pore volume of the BPS-based composite decreases more significantly than that of the HKUST-1@MCM-41 sample. This phenomenon could be associated with the more substantial content of the HKUST-1 component in the HKUST-1@BPS composite. Indeed, HKUST-1 crystallites assist to specific surface area gain, but their abundant location in BPS mesopores results in a total pore volume drop.

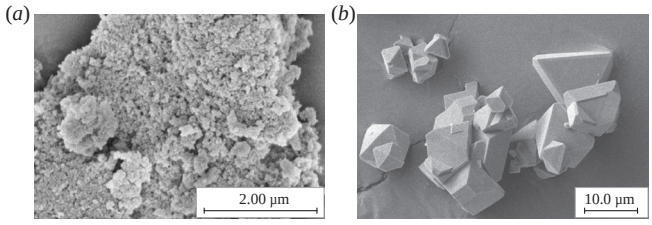


**Figure 2** SEM micrographs of (*a*) BPS and (*b*) the reference HKUST-1 sample synthesized *via* the solvothermal method.

The meso- and micropore volume values in the composites are different. Thus, the HKUST-1@MCM-41 composite is a mesoporous material, while the HKUST-1@BPS adsorbent features a real hierarchical pore structure with almost equal micro- and mesopore contents (Table S2). In the HKUST-1@BPS sample, the two types of mesopores are found corresponding to the maxima in the pore diameter distribution at 1.7 and 17.6 nm, which are a bit lower as compared to the pristine BPS matrix (2 and 7–25 nm). In this case, there are free micropores in the composite. On the contrary, the fraction of micropores in the HKUST-1@MCM-41 material is extremely small, and only the mesopores remain free for gas adsorption. Probably, in the BPS material, HKUST-1 crystallites are mainly located in large mesopores (7–25 nm), blocking them (at least, partially) for guest $N_2$ molecules. This suggestion is supported by a significant (about 2–3 fold) decrease in mesopore diameters as compared to the pristine BPS matrix. In particular, the mesopores with diameters of 3.1 nm are transformed into micropores with diameters of ~ 1.74 nm. The HKUST-1@MCM-41 system has mesopores with sizes of 2.0–5.0 nm, which are only slightly reduced as compared to the pristine MCM-41 matrix. These data indicate a preferential location of HKUST-1 crystallites inside this silica mesopores.

A SEM micrograph of the BPS matrix [Figure 2(*a*)] shows its amorphous nature. It can be seen [Figure 2(*b*)] that the reference HKUST-1 sample obtained by the solvothermal method is composed of large crystals with an average size of ~ 12 μm. In order to understand a morphology evolution of the MOF crystals in the composites, and taking into account that HKUST-1@silica systems were obtained by preliminary joint grinding of $H_3$btc, $Cu^{2+}$ source and silica followed by a solvothermal reaction, the other HKUST-1 sample has been synthesized by the same procedure except a silica addition in the reagent mixture (see Online Supplementary Materials). The SEM micrograph reveals that this reagent pre-treatment almost does not affect an average crystal size of the MOF product (~ 10 μm, Figure S4).

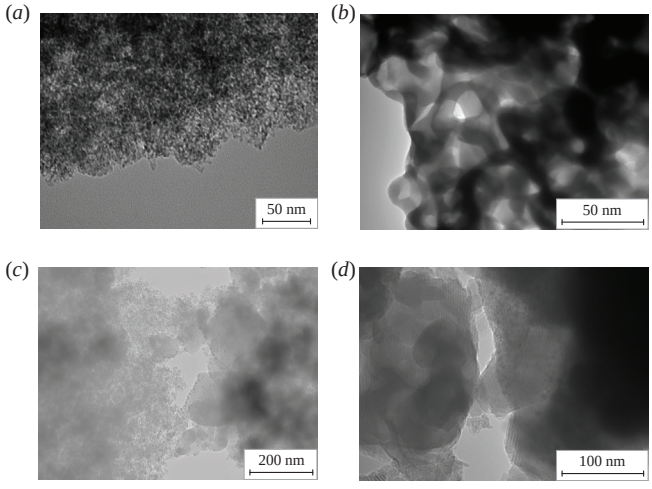


**Figure 3** TEM micrographs of (*a*) BPS, (*b*) MCM-41, (*c*) HKUST-1@BPS and (*d*) HKUST-1@MCM-41 materials.

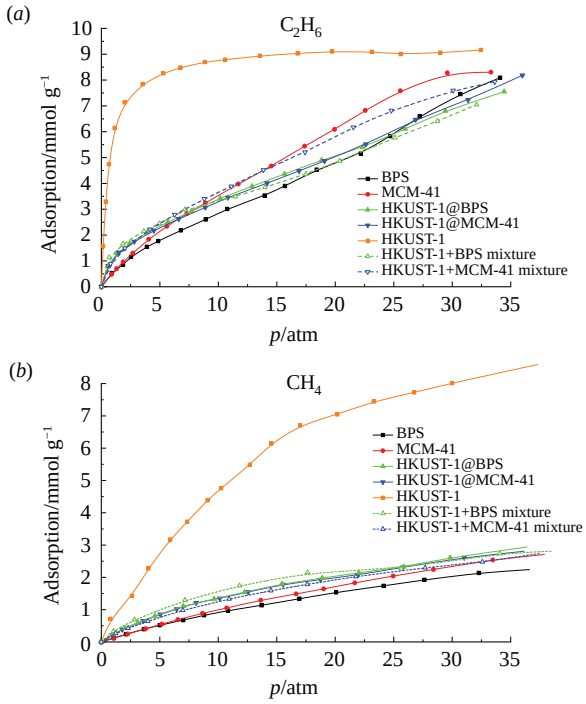


**Figure 4** Adsorption isotherms of (*a*) ethane and (*b*) methane on mesoporous silicas, HKUST-1 and the corresponding composite materials at 298 K, as well as the adsorption isotherms calculated for an idealized mechanical mixture of the components.

The TEM images [Figure 3(*a*),(*b*)] show the differences in microstructures of the silicas, in particular, the large and small mesopores in the BPS matrix, and a regular MCM-41 mesoporous structure [Figure 3(*b*)]. The TEM results reveal the uniform distribution of components in the synthesized HKUST-1@MCM-41 and HKUST-1@BPS composites, thus indicating the formation of homogeneous materials. The average size of HKUST-1 particles embedded in both inorganic matrices is significantly reduced (down to ~ 5–10 nm) as compared to the pristine samples. This decrease could be explained by a confinement effect of the silica frameworks.[23]

The adsorption of methane and ethane on the BPS matrix have been measured for the first time (Figure 4). The HKUST-1 sample shows the highest capacities for both methane and ethane (Table S3). For both gases, the adsorption values determined for the MCM-41 matrix exceed those for BPS by 5–10% under the same conditions (Figure 4, Table S3). The difference between these values is more pronounced for ethane, probably, due to remarkably narrower MCM-41 pores providing close contacts between ethane molecules with silica framework walls, and, thereby, more effective van der Waals adsorbent–adsorbate interactions.[2] A similar effect was observed for selective ethane adsorption on the MUF-15 metal–organic framework with relatively small pores.[24]

The adsorption isotherms for the composites are almost identical and rather similar to those for pristine silica, which confirms a dominating input of an inorganic matrix in adsorption performance. Modification of mesoporous matrices with HKUST-1 crystallites results in a slight increase in methane adsorption as compared to pure silicas. At the same time, the adsorption of ethane on the composites almost does not differ from that of the pristine supports.

The IAST calculations were carried out for a mixture of methane with 10 mol% of ethane, as the closest to natural gas in composition. The data calculated by the IAST method for MCM-41 are consistent with the reported data,[18] where the $C_2H_6/CH_4$ selectivity for a mixture containing 95% $CH_4$ was 7–10 in the pressure range from 1 to 30 atm (264.75 K). The $C_2H_6/CH_4$ selectivity calculated by the

IAST method for MCM-41 is almost independent of pressure, while the selectivity for BPS increases linearly with increasing pressure (Table S4). The highest values of the both ideal and IAST selectivities were obtained for the HKUST-1 sample. The selectivities of pristine MCM-41 and BPS matrices at $p$ = 5 atm are almost identical. For the HKUST-1@MCM-41 and HKUST-1@BPS composites, a rather complex character of selectivity trends is observed. At $p$ = 1 atm, there is a slight increase in the ideal and IAST selectivities for the BPS system. In the case of the MCM-41 matrix, the ideal selectivity decreases slightly as compared to neat MCM-41, but the IAST selectivity increases almost twice. At a pressure increased to 5 atm, the ideal selectivities for both samples decrease significantly, and the IAST selectivity achieves a maximum, which is a typical dependence for the HKUST-1 material.

Thus, the composites based on the microporous HKUST-1 and mesoporous MCM-41 and BPS silicas (HKUST-1@MCM-41 and HKUST-1@BPS) were synthesized by a solvothermal procedure according to the one-step approach. The difference in the pore structure of the pristine silica hosts determines the HKUST-1 content in the produced composites. Thus, the HKUST-1@BPS material contains a bit higher amount of HKUST-1 than the HKUST-1@MCM-41 composite. The composites differ in the pore system, *i.e.*, the HKUST-1@MCM-41 adsorbent is mesoporous, while the HKUST-1@BPS system is hierarchically micro-mesostructured. The adsorption of methane and ethane on the BPS material and produced composites was investigated for the first time in a wide pressure range. At elevated pressures, the IAST selectivity values calculated for the produced composite adsorbents are higher than those calculated for the pristine silicas.

This work may contribute to the development of the practically relevant composite adsorbents based on MOF crystallites and mesoporous silicas for the natural gas purification.

This work was supported by the Russian Foundation for Basic Research under project no. 20-33-90102 in the part related to the adsorption measurements and by the Ministry of Science and Higher Education of the Russian Federation (grant no. 075-15-2021-591) in the part related to the synthesis of adsorbents.

The authors are grateful to the Center for Collective Use of the IOC RAS (Department of Structural Research) for the study of the synthesized adsorbents by electron microscopy.

*Online Supplementary Materials*

Supplementary data associated with this article can be found in the online version at doi: 10.1016/j.mencom.2023.10.026.

## References

1 M. D. Elola and J. Rodriguez, *J. Phys. Chem. C*, 2019, **123**, 30937.
2 F. Anwar, M. Khaleel, K. Wang and G. N. Karanikolos, *Ind. Eng. Chem. Res.*, 2022, **61**, 12269.
3 F. Anwar, K. S. K. Reddy, A. M. Varghese, M. Khaleel, K. Wang and G. N. Karanikolos, *Sep. Purif. Technol.*, 2023, **323**, 124324.
4 H. Yang, L. Xue, X. Yang, H. Xu and J. Gao, *Chin. J. Struct. Chem.*, 2023, **42**, 100034.
5 A. Yu. Tsivadze, O. E. Aksyutin, A. G. Ishkov, A. A. Fomkin, I. E. Men'shchikov, A. A. Pribylov, V. I. Isaeva, L. M. Kustov, A. V. Shkolin and E. M. Strizhenov, *Prot. Met. Phys. Chem. Surf.*, 2016, **52**, 24.
6 I. Senkovska and S. Kaskel, *Microporous Mesoporous Mater.*, 2008, **112**, 108.
7 A. M. Plonka, X. Chen, H. Wang, R. Krishna, X. Dong, D. Banerjee, W. R. Woerner, Y. Han, J. Li and J. B. Parise, *Chem. Mater.*, 2016, **28**, 1636.
8 K. H. Cho, J. W. Yoon, J. H. Lee, J. C. Kim, K. Kim, U.-H. Lee, S. K. Kwak and J.-S. Chang, *Microporous Mesoporous Mater.*, 2020, **307**, 110473.
9 U. Stoeck, I. Senkovska, V. Bon, S. Krause and S. Kaskel, *Chem. Commun.*, 2015, **51**, 1046.
10 U. Stoeck, S. Krause, V. Bon, I. Senkovska and S. Kaskel, *Chem. Commun.*, 2012, **48**, 10841.
11 F.-S. Tang, R.-B. Lin, R.-G. Lin, J. C.-G. Zhao and B. Chen, *J. Solid State Chem.*, 2018, **258**, 346.
12 C. Y. Chuah, S. A. S. C. Samarasinghe, W. Li, K. Goh and T.-H. Bae, *Membranes*, 2020, **10**, 74.
13 P. V. Primakov, G. L. Denisov, V. V. Novikov, O. L. Lependina, A. A. Korlyukov and Y. V. Nelyubina, *Mendeleev Commun.*, 2022, **32**, 105.
14 B. Singh, J. Na, M. Konarova, T. Wakihara, Y. Yamauchi, C. Salomon and M. B. Gawande, *Bull. Chem. Soc. Jpn.*, 2020, **93**, 1459.
15 Z. Li, Y. Zhang and N. Feng, *Expert Opin. Drug Delivery*, 2019, **16**, 219.
16 F. C. de Carvalho, P. F. do Nascimento, M. R. O. de Souza and A. S. Araujo, *Processes*, 2020, **8**, 289.
17 X. Li, J. Yuan, J. Du, H. Sui and L. He, *Ind. Eng. Chem. Res.*, 2020, **59**, 3511.
18 J.-H. Yun, T. Düren, F. J. Keil and N. A. Seaton, *Langmuir*, 2002, **18**, 2693.
19 B. L. Newalkar, N. V. Choudary, P. Kumar, S. Komarneni and T. S. G. Bhat, *Chem. Mater.*, 2002, **14**, 304.
20 M. Ma, L. Lu, H. Li, Y. Xiong and F. Dong, *Polymers*, 2019, **11**, 1823.
21 J. Schell, N. Casas, R. Blom, A. I. Spjelkavik, A. Andersen, J. H. Cavka and M. Mazzotti, *Adsorption*, 2012, **18**, 213.
22 G. S. Deyko, L. M. Glukhov, V. I. Isaeva, V. V. Chernyshev, V. V. Vergun, D. A. Archipov, G. I. Kapustin, O. P. Tkachenko, V. D. Nissenbaum and L. M. Kustov, *Crystals*, 2022, **12**, 279.
23 V. I. Isaeva, V. V. Chernyshev, A. A. Fomkin, A. V. Shkolin, V. V. Veselovsky, G. I. Kapustin, N. A. Sokolova and L. M. Kustov, *Microporous Mesoporous Mater.*, 2020, **300**, 110136.
24 O. T. Qazvini, R. Babarao, Z.-L. Shi, Y.-B. Zhang and S. G. Telfer, *J. Am. Chem. Soc.*, 2019, **141**, 5014.

*Received: 1st June 2023; Com. 23/7179*